

Central Diffraction in ALICE

R. Schicker
for the ALICE collaboration

Phys. Inst., Philosophenweg 12, 69120 Heidelberg, Germany

Abstract. The ALICE experiment consists of a central barrel in the pseudorapidity range $-0.9 < \eta < 0.9$ and of additional detectors covering about 3 units of pseudorapidity on either side of the central barrel. Such a geometry allows the tagging of single and double gap events. The status of the analysis of such diffractive events in proton-proton collisions at $\sqrt{s} = 7$ TeV is presented.

Keywords: Diffraction, Central Production, ALICE, LHC

PACS: 12.38 Aw, 14.40 Be

INTRODUCTION

The ALICE experiment at the Large Hadron Collider (LHC) at CERN consists of a central barrel covering the pseudorapidity range $-0.9 < \eta < 0.9$ and of a muon spectrometer in the range $-4.0 < \eta < -2.4$ [1]. Additional detectors for event classification and trigger purposes exist such that the range $-4.0 < \eta < 5.0$ is covered. The event topologies of single and double gap events can be identified by requiring the existence of charged tracks in the central barrel with absence of activity on one or both sides of the central barrel, respectively.

Approximately 30% of the total proton-proton cross section at the LHC energies is due to diffractive reaction channels, hence detailed measurements of such channels are necessary for a comprehensive understanding of hadron-hadron interactions at high energies. Moreover, central production is dominated by color singlet gluon exchange, hence such an environment offers the possibility to study gluonic degrees of freedom[2].

ALICE DETECTORS

The detector systems of the ALICE central barrel track and identify hadrons, electrons and photons in the pseudorapidity range $-0.9 < \eta < 0.9$. The magnetic field of 0.5 T allows the reconstruction of tracks from very low transverse momenta of about 100 MeV/c to fairly high values of about 100 GeV/c. The main systems for these tasks are the Inner Tracking System (ITS), the Time Projection Chamber (TPC), the Transition Radiation Detector (TRD) and the Time of Flight array (TOF)[3].

Additional detectors are placed on both sides of the central barrel for event classification and for trigger purposes. In particular, an array of scintillator detectors (V0) is placed on both sides and labeled V0A and V0C. These two arrays cover the pseudorapidity range of $2.8 < \eta < 5.1$ and $-3.7 < \eta < -1.7$, respectively.

DATA ANALYSIS

The data taken with a minimum bias trigger in proton-proton collisions at $\sqrt{s} = 7$ TeV have been analyzed according to four event types. Here, the minimum bias trigger is derived by the logical OR at L0 level from the ITS, the V0A and V0C detectors. Gap A and Gap C events are defined by no activity in the V0A or V0C array, respectively. No gap and double gap events are defined by activity or no activity in both V0A and V0C detectors, respectively.

The tracks are reconstructed in the central barrel, and the characteristics of the four classes are compared. The reconstruction of a track is subject to quality criteria such as number of TPC clusters > 65 and subject to rejection of a kink topology in the track.

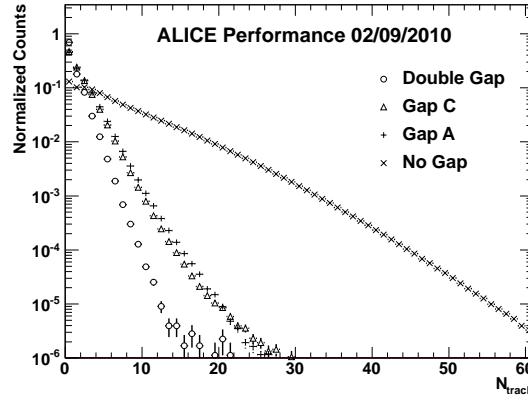


FIGURE 1. Central barrel multiplicity distribution of single, double and no gap events.

Fig. 1 shows the multiplicity of charged tracks in the central barrel for single, double and no gap events. These multiplicity distributions are normalized to unity.

In the following, the four event classes are compared by single and double track observables. Exclusive production of resonances can be selected by choosing events with two tracks in the central barrel, hence only such events are considered in this analysis.

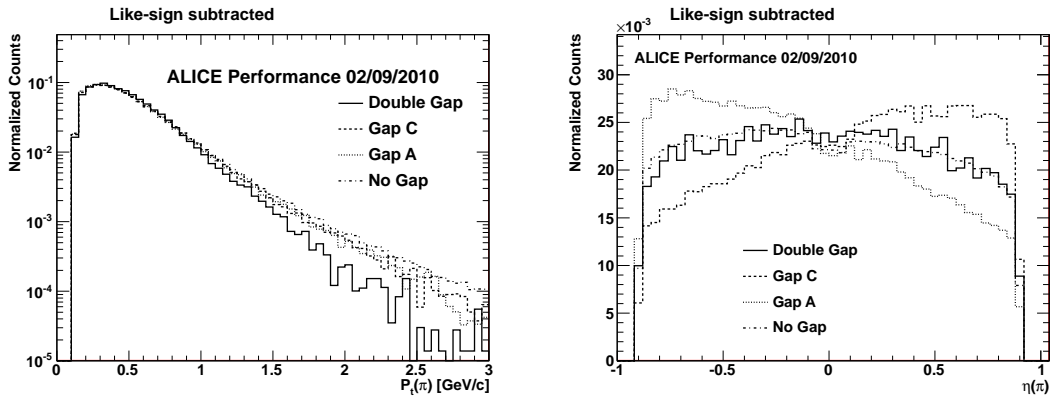


FIGURE 2. Single track transverse momentum distribution (left) and pseudorapidity distribution (right) for single, double and no gap events.

Fig. 2 on the left shows the single track p_T -distribution for single, double and no gap events. Fig. 2 on the right displays the single track pseudorapidity distribution for single, double and no gap events. The distributions shown here are the raw distributions, and are not corrected for efficiencies of detector channels.

In this analysis, the tracks are not particle identified, and all tracks are assumed to be pions. The two track invariant mass carries the information of resonance production.

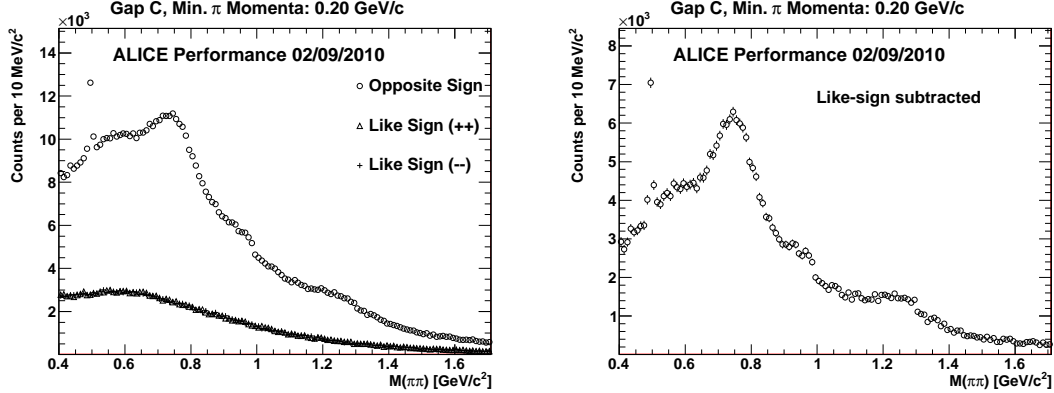


FIGURE 3. Two track invariant mass distribution for gap C events with like-sign background (left) and corrected (right).

Fig. 3 shows the two track invariant mass of gap C events. Here, a single track momentum cut of 0.2 GeV/c is applied. On the left, the distribution of opposite-sign and like-sign pairs is shown. The two like-sign distributions are identical within the size of the data symbols reflecting a charge symmetric acceptance. With a charge symmetric acceptance, uncorrelated tracks contribute equally to opposite-sign and like-sign pairs. The uncorrelated pairs in the opposite-sign spectrum can hence be corrected by subtracting the like-sign spectra. On the right, this like-sign corrected distribution is shown. This like-sign background results in a correction of the raw distribution of about 40%.

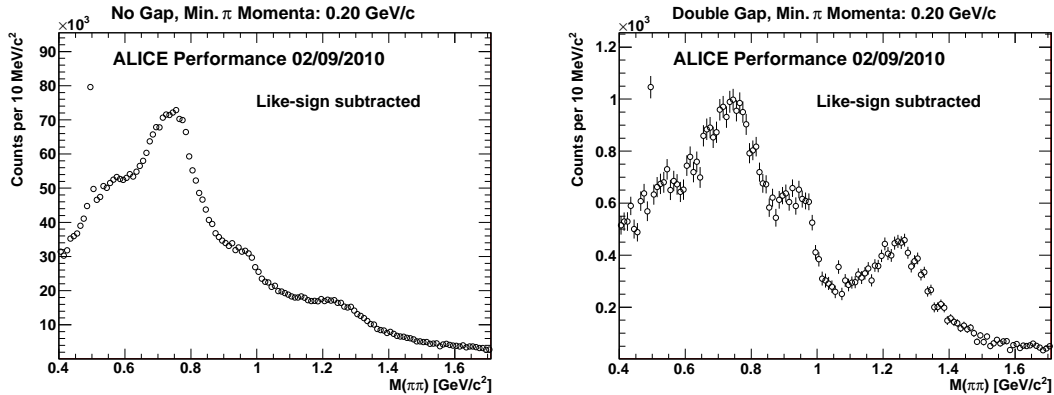


FIGURE 4. Two track invariant mass distribution for no gap events (left) and double gap events (right).

Fig. 4 on the left displays the like-sign corrected mass distribution of no gap events and shows the same qualitative features as Fig. 3. In this event class, the like-sign background results in a correction of about 60% of the raw spectrum. The corrected mass distribution on the left shows a prominent ρ -signal and a K_S^0 signal at 0.5 GeV/c².

The structures at the low mass tail of the ρ are thought to arise from the three body decay $\pi^+\pi^-\pi^0$ of the ω and η -meson. In these decays, only the charged tracks are seen and the π^0 escapes undetected. At the high mass tail, two structures are visible associated with the $f_0(980)$ and the $f_2(1270)$.

Fig. 4 on the right shows the corresponding mass distribution of double gap events. Here, the like-sign background results in a correction of the raw spectrum of about 20%.

The contribution of the $f_0(980)$ and $f_2(1270)$ are quantitatively different in the no gap and double gap events. A normalized invariant mass distribution is defined by dividing the double gap mass distribution by the no gap mass distribution and is shown in Fig. 5.

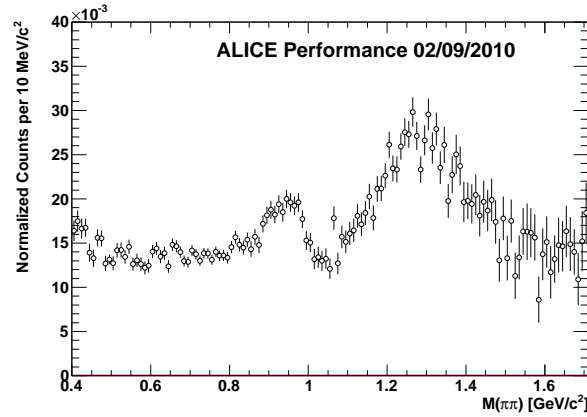


FIGURE 5. Mass distribution of double gap events normalized to no gap events.

Fig. 5 shows structures associated with an enhanced production of the resonances $f_0(980)$ and $f_2(1270)$ in double gap events as compared to no gap events. Such an enhancement of $J^{PC} = J^{++}$ ($J=0,2$) states is evidence that central diffractive production can be tagged by a double gap event topology. The presence of $J^{PC} = 1^{--}$ states such as the ρ in Fig. 4 can be attributed to diffractive double ρ -production with one ρ escaping detection as well as to non-diffractive ρ -production due to detector acceptance. The separation of the ρ -signal into these two sources will be the subject of further studies of double gap events. In particular, the non-diffractive ρ -component will be reduced in the future due to an improved pseudorapidity coverage with a new detector system [4].

ACKNOWLEDGMENTS

This work is supported in part by German BMBF under project 06HD197D and by WP8 of the hadron physics program of the 7th EU program period.

REFERENCES

1. The ALICE collaboration, K. Aamodt et al, The ALICE experiment at the CERN LHC, (2008) JINST_3_S08002
2. F. Close, A. Kirk, G. Schuler, Phys.Lett. B 477 (2000) 13
3. The ALICE Collaboration, J. Alme et al., Nucl. Instrum. Methods A 622 (2010) 316
4. G. Herrera Corral, A new detector array for diffractive physics in ALICE at the LHC, these proceedings